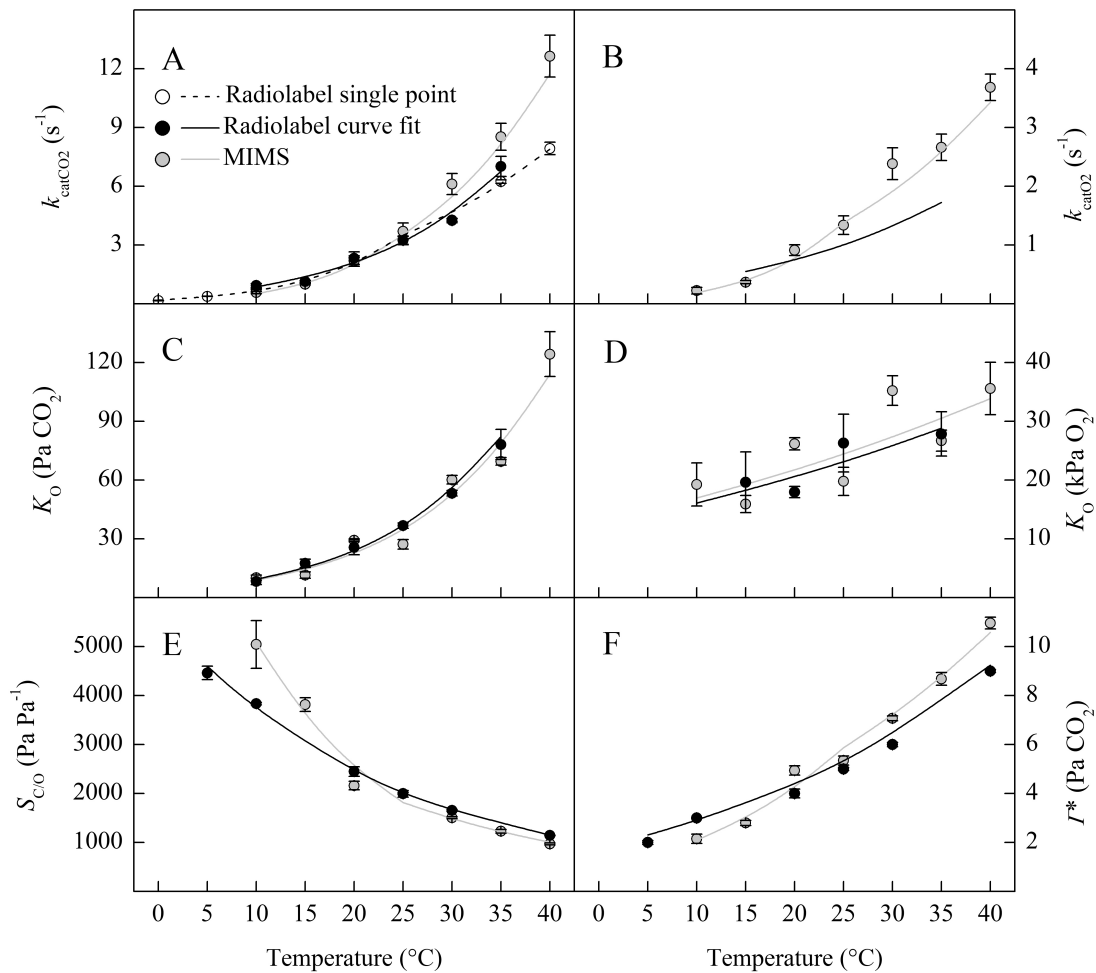


**Title: Temperature response of Rubisco kinetics in *Arabidopsis thaliana*: thermal breakpoints and implications for reaction mechanisms.**

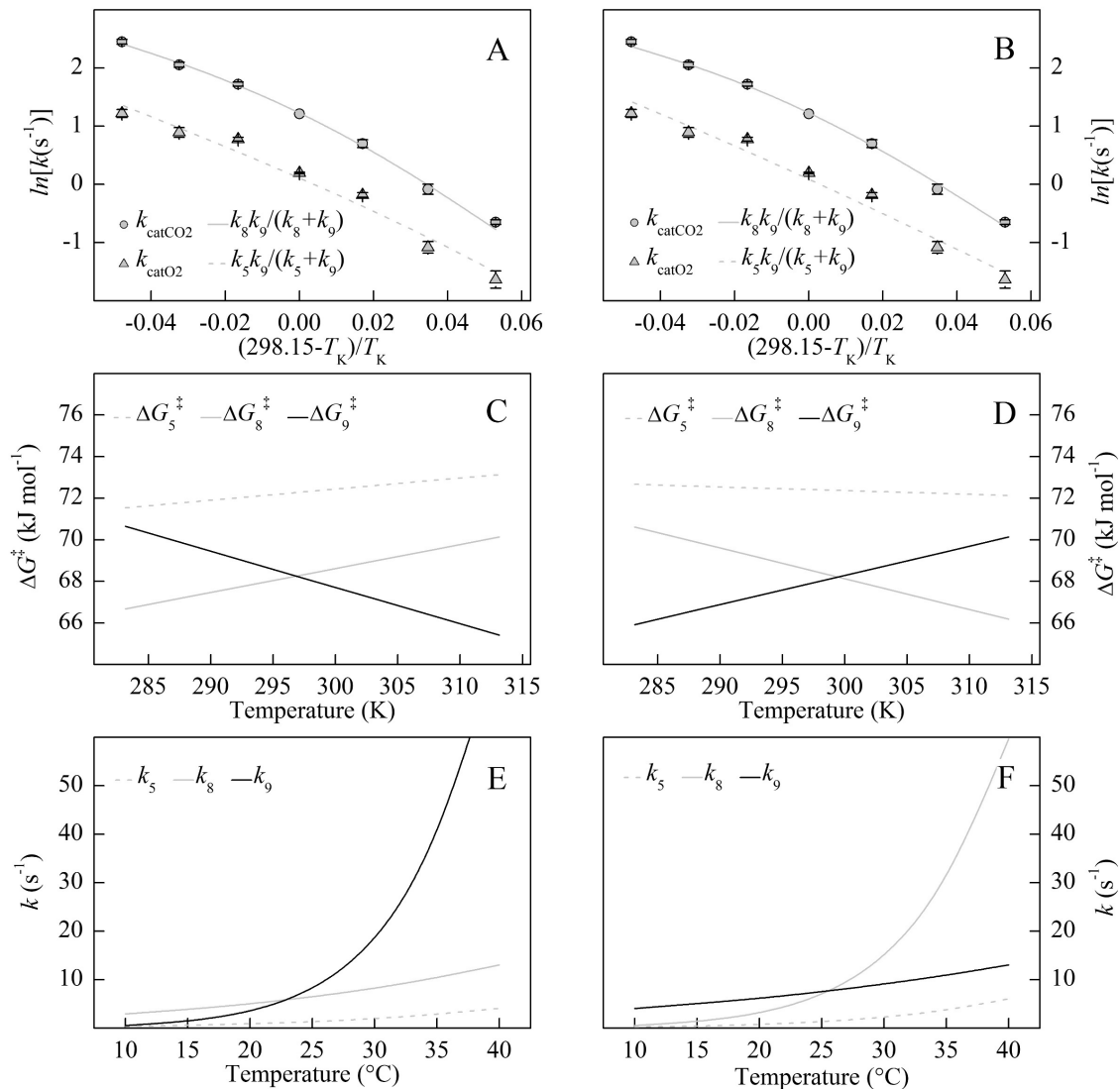
Running title: **Rubisco kinetic thermal breakpoints and reaction mechanisms**

**Authors:** Ryan A. Boyd, Amanda P. Cavanagh, David S. Kubien, Asaph B. Cousins

**Supplementary Figures and Tables**

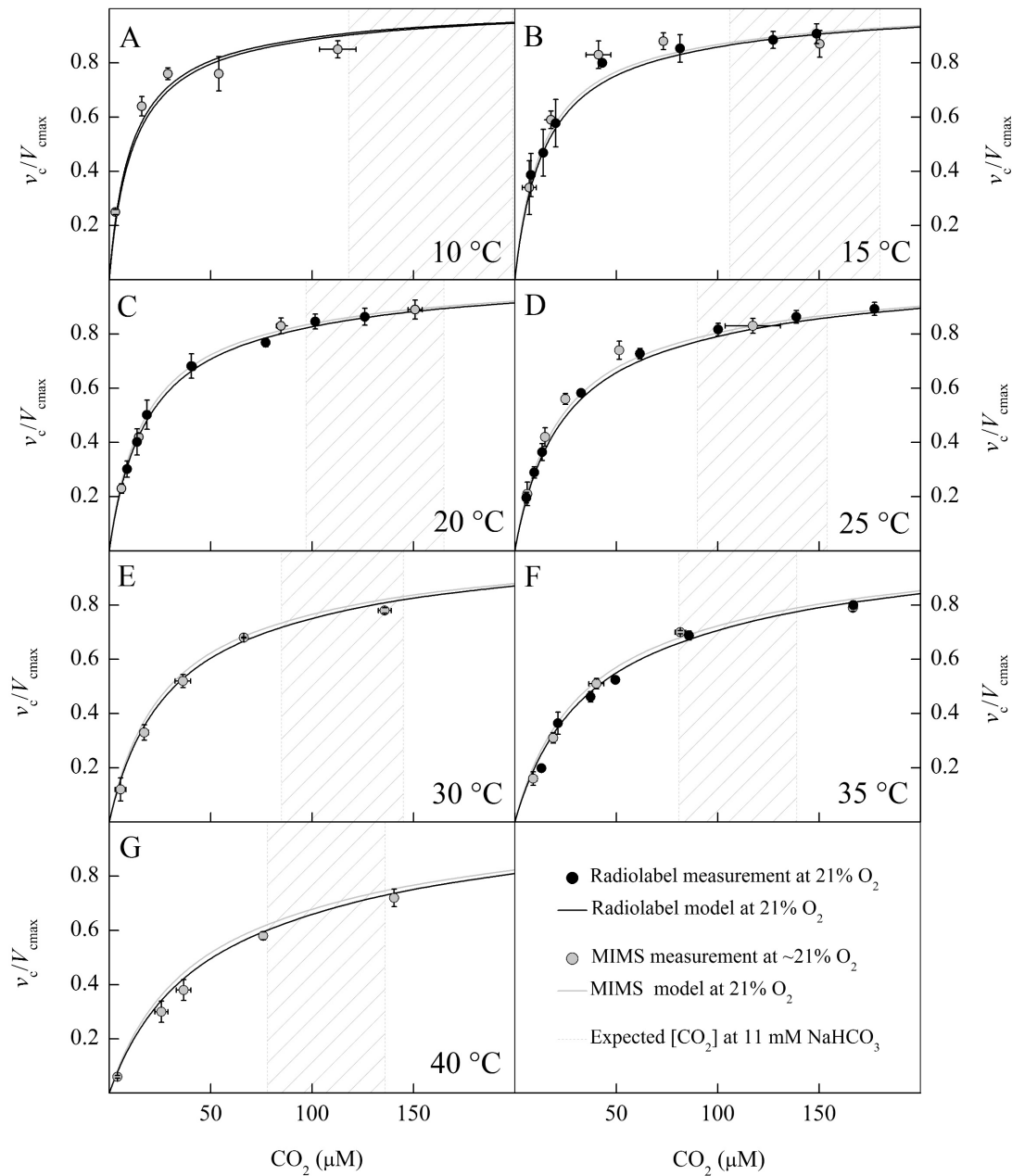


**Supplementary Figure 1.** Temperature response of Rubisco parameters from *Arabidopsis thaliana* measured using radiolabel and MIMS methods compared to previously published *in vivo* method (Walker et al, 2013). The temperature response of catalytic turnover for CO<sub>2</sub> ( $k_{catCO_2}$ , Panel A), and O<sub>2</sub> ( $k_{catO_2}$ , Panel B), the Michaelis constant for CO<sub>2</sub> ( $K_C$ , Panel C), and O<sub>2</sub> ( $K_O$ , Panel D), the specificity for CO<sub>2</sub> over O<sub>2</sub> ( $S_{C/O}$ , Panel E), and the CO<sub>2</sub> compensation point in the absence of dark type respiration ( $\Gamma^*$ , Panel F) are shown.



**Supplementary Figure 2.** Two possible crossover models that result in breakpoints for  $k_{\text{catCO}_2}$  for MIMS data. Each column represents a possible model, for model assumptions see Methods section. The first row shows Arrhenius plots of  $k_{\text{catCO}_2}$  (filled grey circles) and  $k_{\text{catO}_2}$  (filled grey triangles) normalized to zero at 25 °C with model fits  $k_{\text{catCO}_2}$  (solid grey line) and  $k_{\text{catO}_2}$  (dashed grey line). The second row shows the predicted changes in  $\Delta G^\ddagger$  needed for cleavage of the

oxygenated intermediated (step 5, dashed grey line), carboxylated intermediate (step 8, solid grey line), and RuBP enolization (step 9, solid black line). The third row shows the resulting temperature response of the elementary rate constants for steps 5 (dashed grey line), 8 (solid grey line), and 9 (solid black line); this includes the crossover of rates  $k_8$  and  $k_9$  suggested by Badger and Collatz (1977) to cause an observed breakpoint in  $k_{\text{catCO}_2}$ . Note that given the model assumptions, it is arbitrary if  $k_8$  or  $k_9$  is larger at high temperatures therefore both are shown. While this modeling approach results in breakpoints in  $k_{\text{catCO}_2}$ , Arrhenius plots of  $k_{\text{catO}_2}$  remain essentially linear within the measured temperature range (Panel A and B).



**Supplementary Figure 3.** CO<sub>2</sub> response curves from 10 to 40 °C showing measured values from the Radiolabel and MIMS curve fitting methods (filled circles), the predicted response from the modeled  $K_C$  and  $K_O$  values reported in Table 2 using the Michaelis-Menten equation (solid lines), and the predicted CO<sub>2</sub> concentration used in the Radiolabel single point estimate of  $V_{cmax}$

using 11 mM NaHCO<sub>3</sub> (shaded grey box). Because Björkman and Pearcy (1970) suggested that determining the temperature response of  $k_{catCO_2}$  from a single bicarbonate concentration was inhibiting at low temperatures and sub-saturating at high temperatures, the expected CO<sub>2</sub> concentration given 11 mM NaHCO<sub>3</sub> used in the Radiolabel single point  $k_{catCO_2}$  temperature response was calculated (shaded grey boxes). The CO<sub>2</sub> concentration was calculated from the Henderson-Hasselbalch equation  $pH = pK_a + \log_{10}(HCO_3^- / CO_2)$  where pH was 8.2 at all temperatures and the temperature response of pK<sub>a</sub> from Harned and Bonner (1945) was used for pK<sub>a</sub> determined in both 0 and 0.1 M NaCl (Table S4). It was assumed that the only carbon species in solution were CO<sub>2</sub> and the bicarbonate ion such that  $C_{total} = CO_2 + HCO_3^-$  where  $C_{total}$  is the total amount of inorganic carbon and was equal to 11 mM at all temperatures. Because two pK<sub>a</sub> values were used, a range of CO<sub>2</sub> concentrations were calculated at each temperature as indicated by the shaded boxes. The measured values are those measured at approximately 21% O<sub>2</sub> similar to the conditions utilized for the Radiolabel single point estimate of  $V_{cmax}$ . The error bars around the measured values indicate standard error for three biological replicates. In order to compare between measurements, each measured value was divided by the modeled  $V_{cmax}$  so that the y-axis ranges from 0 to 1, representing  $v_c / V_{cmax}$ . To model the predicted  $v_c / V_{cmax}$  response to CO<sub>2</sub>, Henry's Law was used to convert 21% O<sub>2</sub> and the temperature models of  $K_C$  and  $K_O$  reported in pressure from Table 2 to units of concentration, these temperature dependent values were used in the Michaelis-Menten model to calculate  $v_c / V_{cmax}$  for the range of CO<sub>2</sub> concentrations shown. As shown in the figure, when temperature increases 11 mM NaHCO<sub>3</sub> provides less CO<sub>2</sub> indicated by the shaded box moving to lower CO<sub>2</sub> concentrations.



**Supplementary Table 1.** pKa values used in calculations. The second and third columns are pKa values from Harned and Bonner (1945) used to calculate the shaded area in Supplemental Figure 2. The fourth column is the pKa value from Edsell and Wyman (1958) used to calculate CO<sub>2</sub> concentrations for the Radiolabel assay. The fifth column is the measured pKa value determined by MIMS and used in the calculation of CO<sub>2</sub> concentration for the MIMS assay, where the value is the mean of at least three measurements with standard error shown.

<b>Temperature (°C)</b>	<b>0 M NaCl</b>	<b>0.1 M NaCl</b>	<b>Estimated for Radiolabel</b>	<b>Measured for MIMS</b>
10	6.46	6.23	6.36	6.22 ±0.00
15	6.42	6.19	6.30	6.29 ±0.00
20	6.38	6.15	6.25	6.29 ±0.01
25	6.35	6.12	6.23	6.22 ±0.02
30	6.33	6.09	6.21	6.24 ±0.00
35	6.31	6.07	6.19	6.32 ±0.00
40	6.30	6.05	6.19	6.25 ±0.00



**Supplementary Table 2.** Average Rubisco kinetic parameters measured at each temperature with  $\pm$  standard error. The same values are presented in Supplemental Figure 1.

	Radiolabel (curve fit)	Radiolabel (single point)	MIMS
Temperature (°C)	$k_{\text{catCO}_2}$ ( $\text{s}^{-1}$ )		
0		0.2 $\pm$ 0.0	
5		0.4 $\pm$ 0.0	
10	0.9 $\pm$ 0.1	0.7 $\pm$ 0.0	0.6 $\pm$ 0.1
15	1.1 $\pm$ 0.0	1.1 $\pm$ 0.1	1.0 $\pm$ 0.0
20	2.3 $\pm$ 0.3	2.2 $\pm$ 0.3	2.2 $\pm$ 0.2
25	3.2 $\pm$ 0.2	3.2 $\pm$ 0.2	3.7 $\pm$ 0.4
30	4.3 $\pm$ 0.1	4.3 $\pm$ 0.1	6.1 $\pm$ 0.5
35	7.0 $\pm$ 0.5	6.2 $\pm$ 0.1	8.5 $\pm$ 0.7
40		7.9 $\pm$ 0.3	12.6 $\pm$ 1.1
Temperature (°C)	$k_{\text{catO}_2}$ ( $\text{s}^{-1}$ )		
10			0.2 $\pm$ 0.1
15			0.4 $\pm$ 0.0
20			0.9 $\pm$ 0.1
25			1.3 $\pm$ 0.2
30			2.4 $\pm$ 0.3
35			2.7 $\pm$ 0.2
40			3.7 $\pm$ 0.2
Temperature (°C)	$K_C$ (Pa)		
10	8.2 $\pm$ 1.6		10.2 $\pm$ 1.3
15	17.5 $\pm$ 2.2		11.5 $\pm$ 1.6
20	25.6 $\pm$ 3.7		29.2 $\pm$ 0.7
25	36.7 $\pm$ 1.4		27.2 $\pm$ 2.4
30	53.3 $\pm$ 1.4		60.2 $\pm$ 2.2
35	78.2 $\pm$ 7.7		69.5 $\pm$ 1.9
40			124.3 $\pm$ 11.4
Temperature (°C)	$K_O$ (kPa)		
10			19.3 $\pm$ 3.7
15	19.6 $\pm$ 5.2		15.9 $\pm$ 1.5
20	18.0 $\pm$ 1.0		26.2 $\pm$ 1.0
25	26.3 $\pm$ 4.9		19.8 $\pm$ 2.4
30			35.2 $\pm$ 2.5
35	27.9 $\pm$ 3.8		26.7 $\pm$ 1.8
40			35.6 $\pm$ 4.5
Temperature (°C)	$S_{\text{C/O}}$ ( $\text{Pa Pa}^{-1}$ )		
5	4461 $\pm$ 137		
10	3835 $\pm$ 24		5045 $\pm$ 487
15			3816 $\pm$ 138
20	2448 $\pm$ 96		2161 $\pm$ 87
25	2001 $\pm$ 23		1994 $\pm$ 67
30	1655 $\pm$ 22		1505 $\pm$ 21
35			1228 $\pm$ 36
40	1144 $\pm$ 8		971 $\pm$ 21

---

**Supplementary Table 3.** The  $\Delta H^\ddagger$  and  $\Delta S^\ddagger$  calculated for the  $\Delta G^\ddagger$  values presented in

Figure 5 using Equation 18 from the main text.

---

<b>Method</b>	<b>Parameter</b>	<b>Temperature (°C)</b>	<b>Value</b>		
Radiolabel	$\Delta H_3^\ddagger - \Delta H_6^\ddagger$	5 - 40	28.69	±0.52	kJ mol <sup>-1</sup>
	$\Delta S_3^\ddagger - \Delta S_6^\ddagger$	5 - 40	33.04	±1.67	J mol <sup>-1</sup> K <sup>-1</sup>
MIMS	$\Delta H_3^\ddagger - \Delta H_6^\ddagger$	10 - 25	46.67	±4.20	kJ mol <sup>-1</sup>
		25 - 40	36.61	±0.21	kJ mol <sup>-1</sup>
	$\Delta S_3^\ddagger - \Delta S_6^\ddagger$	10 - 25	94.05	±14.33	J mol <sup>-1</sup> K <sup>-1</sup>
		25 - 40	59.75	±0.73	J mol <sup>-1</sup> K <sup>-1</sup>

---

**Supplementary Table 4.** The  $\Delta H^\ddagger$  and  $\Delta S^\ddagger$  calculated for the  $\Delta G^\ddagger$  values presented in

Figure 6 using Equations 16 and 17.

Method	Parameter	Temperature (°C)	value		
Radiolabel	$\Delta H_{kcatCO_2}^\ddagger$	10 - 35	57.21	±3.97	kJ mol <sup>-1</sup>
	$\Delta S_{kcatCO_2}^\ddagger$	10 - 35	-43.63	±13.29	J mol <sup>-1</sup> K <sup>-1</sup>
MIMS	$\Delta H_{kcatO_2}^\ddagger$	10 - 25	87.31	±6.70	kJ mol <sup>-1</sup>
		25 - 40	46.88	±4.20	kJ mol <sup>-1</sup>
	$\Delta S_{kcatO_2}^\ddagger$	10 - 25	50.85	±22.34	J mol <sup>-1</sup> K <sup>-1</sup>
		25 - 40	-84.61	±42.84	J mol <sup>-1</sup> K <sup>-1</sup>
	$\Delta H_{kcatCO_2}^\ddagger$	10 - 25	86.93	±1.79	kJ mol <sup>-1</sup>
		25 - 40	60.22	±2.05	kJ mol <sup>-1</sup>
	$\Delta S_{kcatCO_2}^\ddagger$	10 - 25	57.61	±6.75	J mol <sup>-1</sup> K <sup>-1</sup>
		25 - 40	-31.90	±6.00	J mol <sup>-1</sup> K <sup>-1</sup>

**Supplementary Table 5.** The  $\Delta H^\ddagger$  and  $\Delta S^\ddagger$  calculated for the  $\Delta G^\ddagger$  values presented in Figure 7 using Equations 9 through 15 from the main text.

Method	Temperature (°C)	Step	$\Delta H^\ddagger$ (kJ mol <sup>-1</sup> )	$\Delta S^\ddagger$ (J mol <sup>-1</sup> K <sup>-1</sup> )
Radiolabel	10 - 35	3	24.2 ±3.9	-154.6 ±13.0
		5	37.8 ±8.3	-116.9 ±26.2
		6	-5.9 ±3.9	-244.2 ±13.0
		8	-- --	-38.7 ±13.2
		9	57.2 ±3.9	-37.2 ±13.2
		10	-- --	-30.2 ±13.2
MIMS	10 - 25	3	77.0 ±38.8	25.4 ±13.4
		5	92.0 ±7.7	67.5 ±26.1
		6	33.0 ±3.3	-111.4 ±10.8
		8	101.5 ±2.9	110.8 ±9.5
		9	61.0 ±1.5	-23.5 ±5.3
		10	-- --	-16.5 ±5.3
	25 - 40	3	23.2 ±6.0	-155.2 ±19.6
		5	45.1 ±3.1	-89.9 ±10.5
		6	-11.6 ±6.1	-261.0 ±20.0
		8	-- --	-25.1 ±5.3
		9	61.0 ±1.5	-23.5 ±5.3
		10	-- --	-16.5 ±5.3